JOURNAL OF MATERIALS SCIENCE 12 (1977) 2214–2222

Computer simulation of impression creep by the finite element method

HSIANG-YUNG YU, J. C. M. LI
Materials Science Program, Department of Mechanical and Aerospace Sciences, University of Rochester, Rochester, New York, USA

The steady state impressing velocity of the punch during an impression creep test is calculated by the finite element method based on a single power law constitutive equation for the deformation of each and every element. The calculated impressing velocities and their stress dependence agree very well with the experimental values on succinonitrile crystals using empirical power laws obtained from unidirectional creep tests.

1. Introduction

In a preceding paper*, a new creep test is introduced. It is a modified indentation test with a cylindrical flat-end indenter. A steady-state velocity is observed in this new test, which has the same stress and temperature dependences as conventional creep tests using bulk specimens. Two mechanisms have been analysed; bulk diffusion and surface diffusion. A third mechanism, dislocation creep, is analysed in this paper by the finite element method. The results are compared with experiments on succinonitrile crystals.

Finite element method has been used widely in engineering applications [1, 2], mainly because of the availability of large-memory computers. The principle involved is very simple. The system is divided into a number of volume elements in the form of polyhedrons, or other well defined shapes. The corners of the polyhedrons, or the nodes, are to assume new positions under prescribed boundary conditions. The compatibility requirements are fulfilled automatically if the polyhedral shapes are retained for each element. Stress and strain may not be continuous at the boundaries between the elements. Instead, equilibrium or steady-state conditions are established by minimizing certain quantities such as the potential energy for elastic equilibrium.

The incremental procedure used by Greenbaum and Rubinstein [3], somewhat modified and corrected, was adopted for this work. The following assumptions were made: (1) The material is isotropic and homogeneous; (2) the system is isothermal; (3) a power law creep equation is applicable to each and every element; (4) displacements and strains are small so that small deformation theory is applicable; (5) the displacement at any point inside an element is a linear function of the cylindrical co-ordinates of that point.

2. The element, displacement, and strain

For the present axi-symmetric problem, the convenient shape of the element is a volume of revolution of triangular cross-section, as shown in Fig. 1. Because of the axi-symmetry, the nodal points i, j, k can move in only two dimensions; hence the problem becomes two dimensional. The displace-

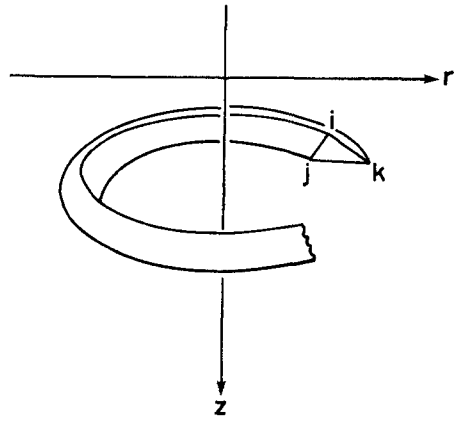

Figure 1 An element in an axi-symmetric solid.

* S. N. G. CHU and J. C. M. LI, *J. Mater. Sci.* **12** (1977) 2200.

ment of each node has two components, u_i in the r-direction and w_i in the z-direction. Hence for each element, six components of the three nodal displacements define completely the position of the element. Let $\{\delta\}$ be a column vector of these components. Its transpose is

$$\{\delta\}^T = \{u_i, w_i, u_j, w_j, u_k, w_k\}. \quad (1)$$

The displacement at any point (r, z) inside the element is assumed to be a linear function of r and z. This assumption assures that the triangular shape is retained all the time so that the elements remain compatible to each other. The linear function can be determined from the co-ordinates r_i, z_i, etc. of the three nodal points and $\{\delta\}^T$. It can be easily shown that the two-component displacement vector $\{\delta^*\}^T = \{u, w\}$ at (r, z) is

$$\{\delta^*\} = [L]\{\delta\} \quad (2)$$

where $[L]$ is a 2 x 6 matrix,

$$[L] = \frac{1}{\beta}\begin{bmatrix} L_i & 0 & L_j & 0 & L_k & 0 \\ 0 & L_i & 0 & L_j & 0 & L_k \end{bmatrix}, \quad (3)$$

with

$$\beta = \begin{vmatrix} 1 & r_i & z_i \\ 1 & r_j & z_j \\ 1 & r_k & z_k \end{vmatrix}, \quad L_i = \begin{vmatrix} 1 & r & z \\ 1 & r_j & z_j \\ 1 & r_k & z_k \end{vmatrix}, \text{ etc.} \quad (4)$$

Note that L_i, etc. contain the co-ordinates (r, z).

Knowing the displacements at any point, the strain components at (r, z) can be obtained by differentiation;

$$\{\varepsilon\} \equiv \begin{Bmatrix} \epsilon_{zz} \\ \epsilon_{rr} \\ \epsilon_{\theta\theta} \\ \epsilon_{rz} \end{Bmatrix} \equiv \begin{Bmatrix} (\partial w/\partial z)_r \\ (\partial u/\partial r)_z \\ u/r \\ (\partial u/\partial z)_r + (\partial w/\partial r)_z \end{Bmatrix}. \quad (5)$$

It is seen that all components of strain except $\epsilon_{\theta\theta}$ are uniform within the element. Note that the shear strain is "engineering" rather than tensorial, and that the strain is overall and can include creep strain.

Substituting Equation 2 into Equation 5 gives

$$\{\varepsilon\} = [B]\{\delta\} \quad (6)$$

where $[B]$ is the following 4 x 6 matrix:

$$[B] = \frac{1}{\beta}\begin{bmatrix} 0 & r_k - r_j & 0 & r_i - r_k & 0 & r_j - r_i \\ z_j - z_k & 0 & z_k - z_i & 0 & z_i - z_j & 0 \\ L_i/r & 0 & L_j/r & 0 & L_k/r & 0 \\ r_k - r_j & z_j - z_k & r_i - r_k & z_k - z_i & r_j - r_i & z_i - z_j \end{bmatrix} \quad (7)$$

3. The stress and the potential energy

Since the total strain $\{\varepsilon\}$ may contain creep strain $\{\varepsilon^c\}$, the elastic strain at (r, z) is

$$\{\varepsilon^E\} = \{\varepsilon\} - \{\varepsilon^c\}, \quad (8)$$

from which the stress components can be obtained from linear elasticity:

$$\{\sigma\} \equiv \begin{Bmatrix} \sigma_{zz} \\ \sigma_{rr} \\ \sigma_{\theta\theta} \\ \sigma_{rz} \end{Bmatrix} = \frac{2\mu}{1-2\nu}\begin{bmatrix} 1-\nu & \nu & \nu & 0 \\ \nu & 1-\nu & \nu & 0 \\ \nu & \nu & 1-\nu & 0 \\ 0 & 0 & 0 & (1-2\nu)/2 \end{bmatrix} \times \{\varepsilon^E\} \equiv [D]\{\varepsilon^E\}, \quad (9)$$

where μ and ν are shear modulus and Poisson's ratio respectively.

The potential energy of the system is defined as its strain energy minus the external work done on the system. In the present case, it is the strain energy of all the elements minus the external work done by the punch, namely

$$U = \tfrac{1}{2}\sum_1^{\alpha}\int_V \{\varepsilon^E\}^T[D]\{\varepsilon^E\}dV - \sum_1^{\beta}\int_S \{\sigma_a\}^T\{\delta^*\}dS \quad (10)$$

where α is the total number of elements, V is the volume of each element, β is the number of those elements directly under the punch, and $\{\sigma_a\}^T \equiv \{0, \sigma_z\}$ is a two-component vector of surface stress applied by the punch over the surface S of each of these elements.

The potential energy can be minimized with respect to all the nodal displacements. Let N be the total number of nodes, Equation 10 is a function of $2N$ variables. However, the expression is in a form convenient for differentiation with respect to the nodal displacements of each element, namely, 6α variables, but under the obvious constraint that all common nodes must have the same displacements. By using the 6α variables, the equilibrium conditions can be obtained by introducing $6\alpha - 2N$ Lagrange indeterminate multipliers. By

substituting Equations 2, 6, and 8, Equation 10 can be differentiated to give, holding creep strain constant,

$$dU = \sum^{\alpha} \left[\int_V \{\delta\}^T [B]^T [D] [B] \, dV - \int_V \{\varepsilon^c\}^T [D] [B] \, dV - \int_S \{\sigma_a\}^T [L] \, dS - \{M\}^T \right] d\{\delta\} \quad (11)$$

where $\{M\}$ is a 6×1 column matrix of the six Lagrange multipliers. The constraint of identical displacements at a common node requires that the multipliers at each node add up to zero. The potential energy is a minimum when the 1×6 matrix of the bracket of Equation 11 is zero. The surface integral in Equation 11 applies only to those elements under the punch, that is $\{\sigma_a\}^T = \{0, 0\}$ for all elements except the ones directly under the punch. Let

$$[K] = \int_V [B]^T [D] [B] \, dV \quad (12)$$

$$\{F^c\} = \int_V [B]^T [D] \{\varepsilon^c\} dV \quad (13)$$

$$\{F^a\} = \int_S [L]^T \{\sigma_a\} dS \quad (14)$$

$$\{F\} = \{M\} + \{F^a\} + \{F^c\} \quad (15)$$

where the 6×1 column vectors $\{F^c\}$ and $\{F^a\}$ can be considered as creep forces and applied forces respectively, as if they are exerted on the nodes. Then the equilibrium condition is simply

$$[K]\{\delta\} = \{F\} \quad (16)$$

for each element. However, because of the indeterminate multipliers, the equilibrium conditions for the elements are difficult to solve directly but can be assembled into a set of $2N$ equations for the whole body (N = number of nodes):

$$[K]_b \{\delta\}_b = \{F\}_b \quad (17)$$

where $[K]_b$ is a $2N \times 2N$ stiffness matrix and $\{\delta\}_b$ and $\{F\}_b$ are $2N \times 1$ displacement and nodal-force column vectors respectively. Then the multipliers add up to zero at each common node and there are no multipliers for isolated nodes. The problem becomes a simple matrix inversion scheme directly solvable by a computer without iteration.

4. Power law of creep

So far the creep strain has been held constant in minimizing the potential energy; determining creep strain from stress is an unsolved problem in plasticity. For unidirectional creep tests, the creep rate is generally found to be a power law of stress, namely

$$\Delta\epsilon_e^c = A\sigma_e^n \Delta t \quad (18)$$

where A and n are constants at constant temperature, $\Delta\epsilon_e^c/\Delta t$ is the creep rate, and σ_e is the unidirectional stress. The creep compliance is usually defined as

$$\frac{\Delta\epsilon_e^c}{\sigma_e} = A\sigma_e^{n-1} \Delta t. \quad (19)$$

For the triaxial situation within each element, the creep compliance still can be calculated by Equation 19 except that σ_e is replaced by the equivalent creep stress of the von Mises criterion

$$\sigma_e = [(\sigma_{rr} - \sigma_{\theta\theta})^2 + (\sigma_{\theta\theta} - \sigma_{zz})^2 + (\sigma_{zz} - \sigma_{rr})^2 + 6\sigma_{rz}^2]^{1/2}/\sqrt{(2)}. \quad (20)$$

The following incremental flow rule is then used to calculate other creep strains:

$$\{\Delta\varepsilon^c\} = \frac{A}{2}\sigma_e^{n-1} \begin{bmatrix} 2 & -1 & -1 & 0 \\ -1 & 2 & -1 & 0 \\ -1 & -1 & 2 & 0 \\ 0 & 0 & 0 & 6 \end{bmatrix} \{\sigma\} \, \Delta t \quad (21)$$

Note that since $\sigma_{\theta\theta}$ is not uniform within the element, neither are σ_e and $\{\Delta\varepsilon^c\}$. However, $\{\Delta\bar{\varepsilon}^c\}$ can be calculated if $\{\bar{\sigma}\}$ at the centroid of the triangle is used in Equation 21.

5. Approximations and programming

The stiffness matrix for each element, Equation 12 can be approximated by using an average $[B]$, namely, by replacing (r, z) with $(\bar{r}, \bar{z})$ the coordinates of the centroid of the triangle. Then $\bar{L}_i = \bar{L}_j = \bar{L}_k = \beta/3$. Let this average $[B]$ be $[\bar{B}]$. The stiffness matrix is then simply

$$[K] = \pi\bar{r}|\beta|[\bar{B}]^T [D] [\bar{B}] \quad (22)$$

where β is given by Equation 4 and is twice the area of the triangle. Although β may be $\pm$ depending on the order of ijk, the area of the triangle is posi-

tive always. Similarly the creep force can be approximated by

$$\{\mathbf{F}^c\} = \pi\bar{r}|\beta|[\bar{B}]^T[D]\{\Delta\bar{\varepsilon}^c\} \qquad (23)$$

where $\{\Delta\bar{\varepsilon}^c\}$ is calculated from Equation 21 at the centroid of the triangle for a certain time period Δt to be assigned later.

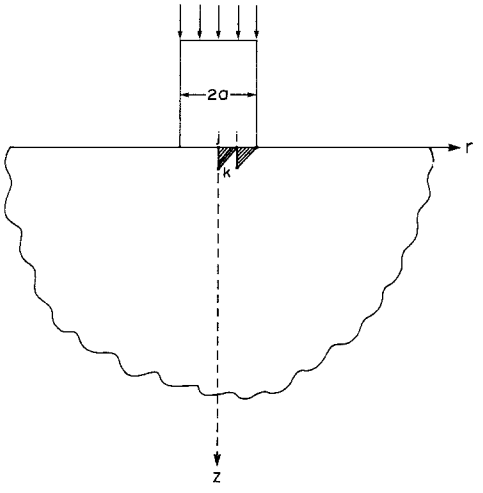

Figure 2 The boundary elements over which the external load is applied.

Since the surface force, Equation 14 applies only to the elements directly under the punch as shown in Fig. 2, two of the nodal points such as i and j have the same z co-ordinate. Integration over the stressed surface gives

$$\{\mathbf{F}^a\}^T = \frac{\pi}{3\beta}\{0, N_i, 0, N_j, 0, 0\}, \qquad (24)$$

where

$$N_i = (r_i - r_j)^2(z_i - z_k)(2r_i + r_j)\sigma_z \qquad (25)$$

and

$$N_j = (r_i - r_j)^2(z_i - z_k)(r_i + 2r_j)\sigma_z \qquad (26)$$

The programming procedure is as follows: At time zero, the elastic stresses are determined by using Equation 17 for the whole system without the creep force. The $2N \times 2N$ stiffness matrix is assembled, using Equation 22 for each element. For a given σ_z, the external force is calculated by Equation 24 for each element and assembled into a $2N \times 1$ column vector. The solution of Equation 17 is by matrix inversion. From the displacements of the nodes, strain can be calculated from Equation 6 and stress from Equation 9. As discussed earlier, average values can be obtained by using centroid co-ordinates.

The elastic stresses calculated are assumed constant for the next time increment Δt. The creep strain is obtained by Equation 21 knowning the unidirectional creep law of Equation 18. Then the creep force is calculated by Equation 23 which can be assembled into a $2N \times 1$ column vector. The incremental displacement due to this creep force is again solved by Equation 17 using matix inversion. Such incremental displacement produces punch motion, as well as an incremental total strain given by Equation 6, from which the elastic part is given by Equation 8. The incremental stress calculated by Equation 9 is then added to the stress at time zero. This incremental stress should be smaller than the starting elastic stress to justify the constant stress assumption for the time interval Δt. If not, the interval Δt should be reduced. The procedure is then repeated for the next time interval.

According to Sutherland [4], the maximum time interval at any stage must be such that the incremental creep strain given by Equation 18 is not greater than the elastic strain. In other words, the creep compliance should be smaller than the elastic compliance of the matrial. Otherwise, the procedure may become unstable. In the present case, the first time interval is calculated by

$$\Delta t_1 = \zeta_0/2\mu(1+\nu)A(\sigma_e)_{max}^{n-1} \qquad (27)$$

where ζ_0 is set equal to 0.1. Subsequent intervals are calculated by

$$\Delta t_{i+1} = \zeta_i(\Delta t)_i(\sigma_e/\Delta\sigma_e)_{min} \qquad (28)$$

where ζ_i is again set equal to 0.1. Furthermore $\Delta t_{i+1}/\Delta t_i$ has an upper limit of 2 to assure convergence of the calculation. A schematic diagram for the program is shown in Fig. 3.

6. Results on succinonitrile crystals

The arrangement of the elements is shown in Fig. 4, as cross-sections of the volumes of revolution. The radius of the punch is a. The specimen has a diameter of $64a$ and a length of $72a$. There are 186 elements and 113 nodes.

To test the program, the elastic stress field is calculated first. From the elastic constants and their temperature dependences reported by Fontaine and Moriamez [5] for single crystals, a set of isotropic constants are calculated by using both Voigt and Reuss averages [6], and is found to be $\mu = 6.83 \times 10^8\ \mathrm{N\,m^{-2}}$ and $\nu = 0.416$ at 37° C. The two averages turn out to be almost identical. The computed zz component of stress

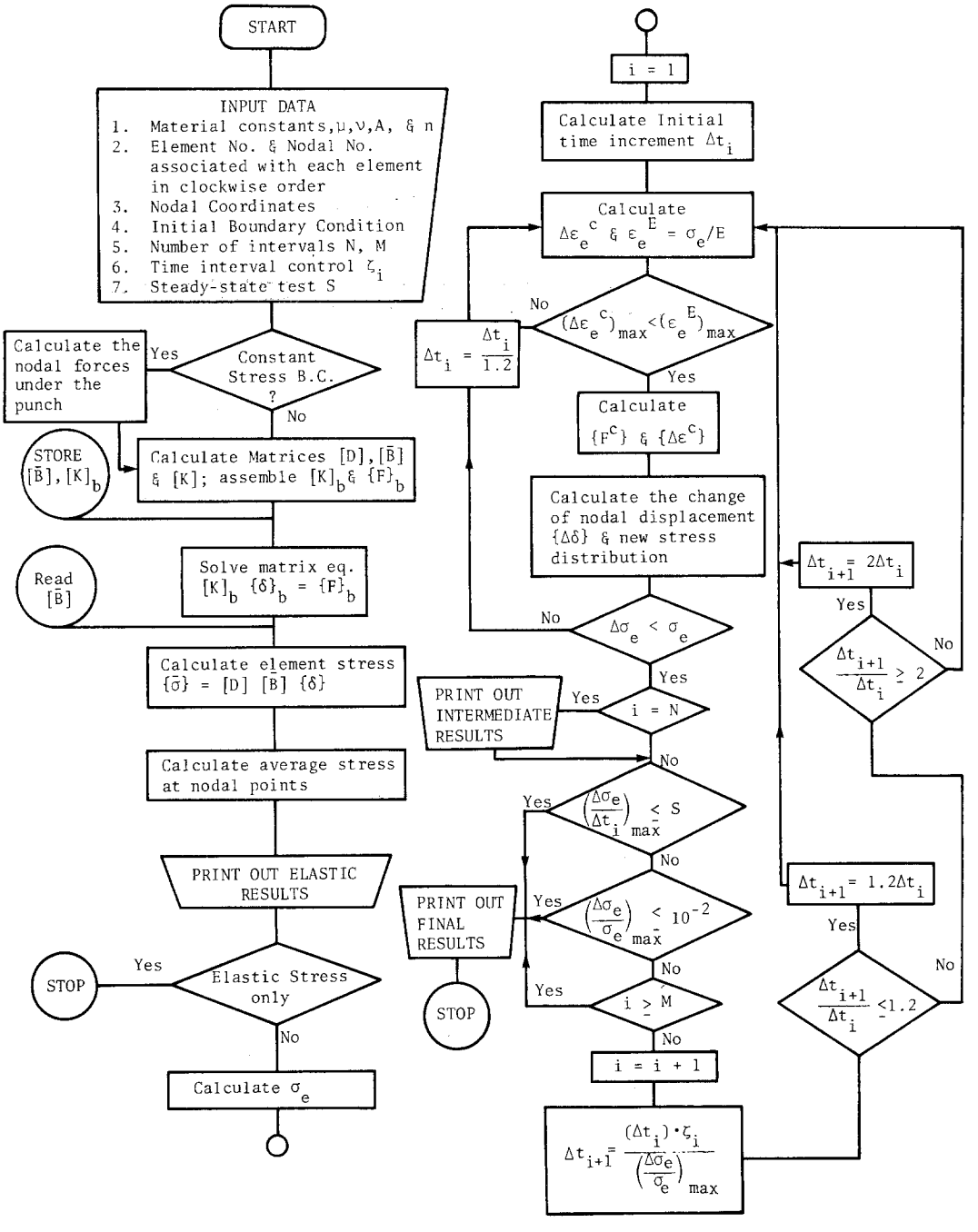

Figure 3 The flow chart for the impression creep computer program.

along the z-axis is compared with theoretical values and is shown in Fig. 5. For the uniform-stress boundary condition under the punch, the elastic problem was solved by Terazawa [7] for the semi-infinite medium. The zz stress along the z-axis is given by

$$\frac{\sigma_{zz}}{\sigma} = 1 - \frac{z^3}{(z^2 + a^2)^{3/2}} \tag{29}$$

where σ is the punching stress. For the uniform-displacement boundary condition under the punch, the elastic problem was solved by Härding and Sneddon [8], also for the semi-infinite medium. In this case the zz stress along the z-axis is given by

$$\frac{\sigma_{zz}}{\sigma} = \frac{(3z^2 + a^2)a^2}{2(z^2 + a^2)^2} \tag{30}$$

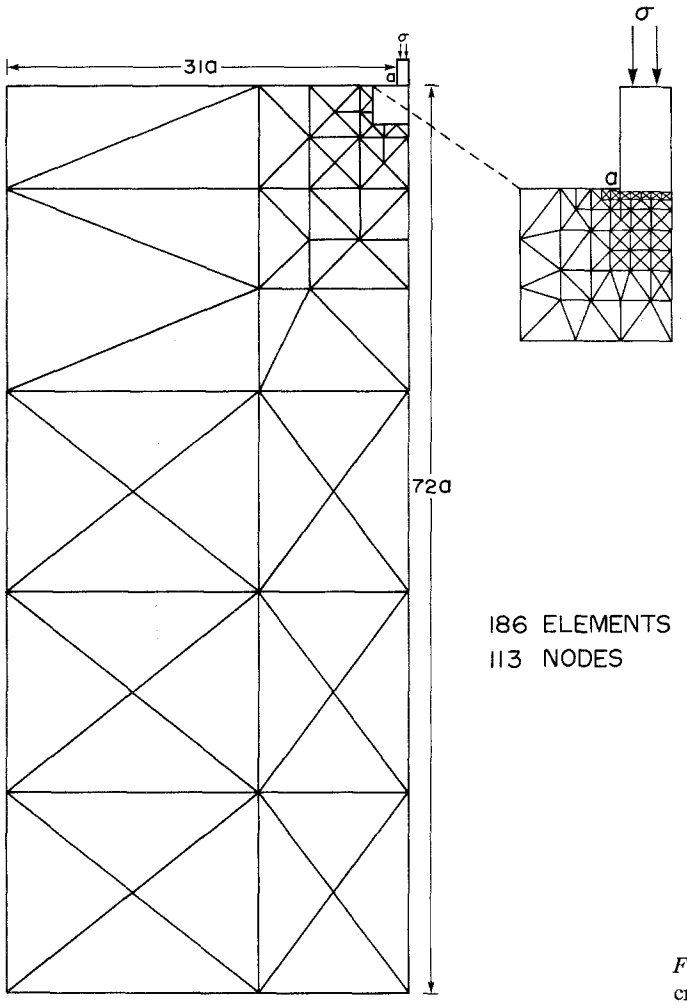

Figure 4 The layout of elements for impression creep analysis.

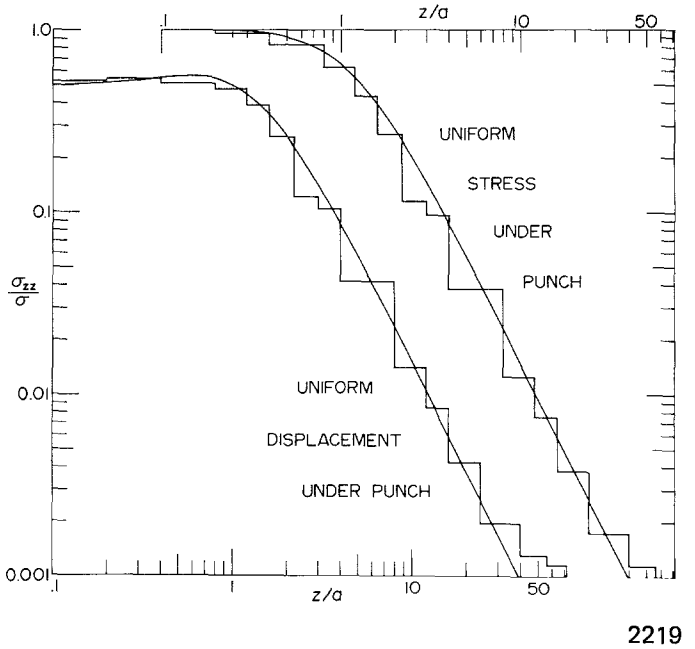

Figure 5 A comparison between calculated and theoretical stresses under punch.

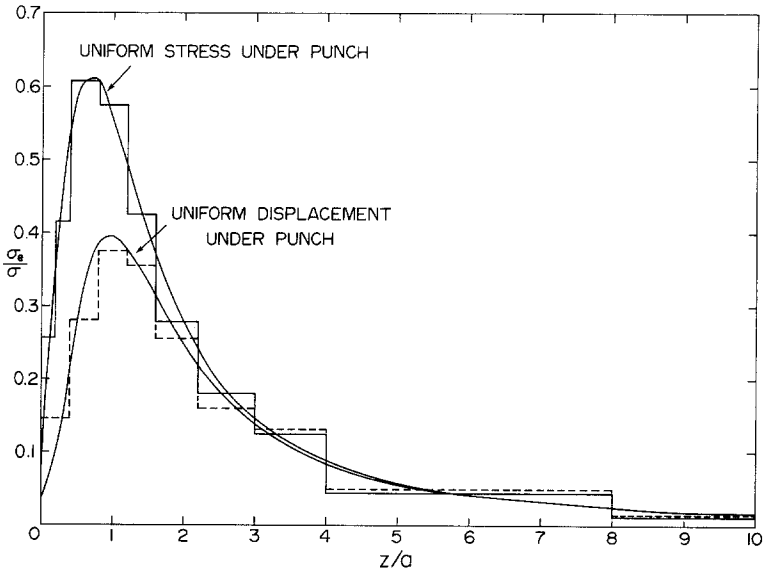

Figure 6 The von Mises stresses under punch.

Equations 29 and 30 are plotted in Fig. 5 as curves with a factor of 4 displaced from each other on the z/a axis for clarity. Although at $z = 0$, Equation 29 gives 1 and Equation 30 gives 0.5, both approach $3a^2/2z^2$ for large z. Note also that while Equation 29 is monotonic, Equation 30 has a maximum value of 9/16 at $a^2/z^2 = 3$. The agreement between equations and the computed values, as shown in Fig. 5, provides some support for the validity of both the computer program and the finite element layout.

Since the Von Mises stress is the cause of creep, its variation along the z-axis is shown in Fig. 6. It turns out to be the same as twice the maximum shear stress ($\sigma_{rr} = \sigma_{\theta\theta}$, $\sigma_{rz} = 0$). The curves are the theoretical values of Terazawa [7] (uniform-stress boundary condition).

$$\frac{\sigma_e}{\sigma} = \frac{1-2\nu}{2} - \frac{z[(1-2\nu)z^2 - 2(1+\nu)a^2]}{2(z^2+a^2)^{3/2}} \tag{31}$$

and those of Harding and Sneddon [8] (uniform-displacement condition):

$$\frac{\sigma_e}{\sigma} = \frac{[(7-2\nu)z^2 + (1-2\nu)a^2]a^2}{4(z^2+a^2)^2} \tag{32}$$

By using $\nu = 0.416$ they are included in Fig. 6 for comparison. While at $z = 0$, one approaches $(1 - 2\nu)/2$ and the other $(1 - 2\nu)/4$, they both approach $(7 - 2\nu)a^2/4z^2$ at large z.

It is seen from Fig. 6 that, for both the uniform-stress boundary condition and the uniform-displacement boundary condition, the maximum Von Mises stress is not located directly underneath the punch but at a distance below it approximately equal to the radius of the punch. This suggests that deformation is the most severe not at the punch–sample interface but within the material. As a result, the punch–sample interfacial structure is not as important as in the case of conventional compression creep.

Now to compute the impression creep; the power law constitutive equation was obtained from conventional compression tests reported in the previous paper. The results give Equation 18 with $A = 0.84$ and $n = 4$, when σ_e is in MN m^{-2} and Δt in seconds. These and the elastic constants are all the materials properties needed for the computation of punch velocity. The program started by using a constant and uniform σ_z (the punching stress) over all the elements under the punch. The

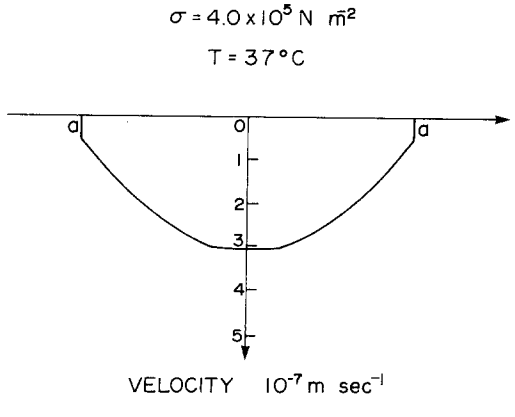

Figure 7 Velocity profile under punch for uniform-stress boundary condition.

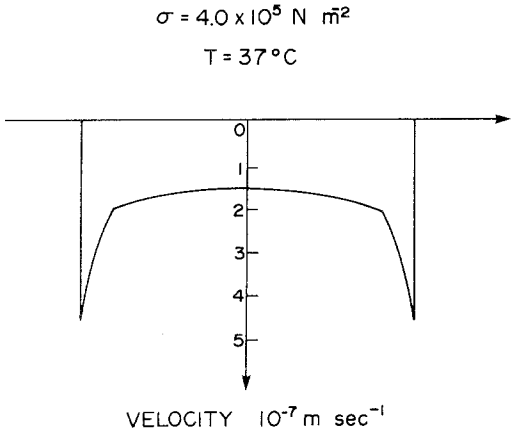

Figure 8 Velocity profile under punch for initially uniform-displacement boundary condition and constant local stress during creep.

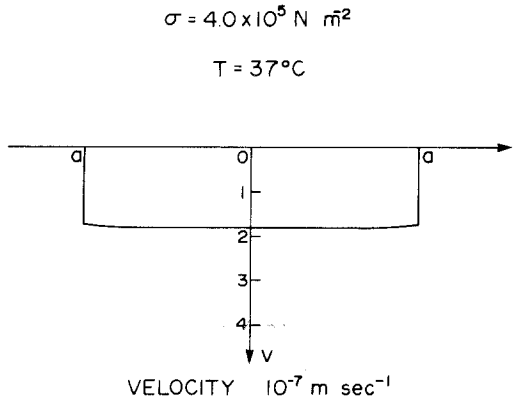

Figure 9 Velocity profile under punch by using average nodal forces of the two previous boundary conditions.

velocity profile obtained is shown in Fig. 7, and is not the experimental condition. This result indicates that the stress under the punch is not uniform during creep. A stress distribution based on uniform displacement under the punch at time zero and held constant during creep gives a velocity profile shown in Fig. 8, which is again not the experimental condition. However, an inspection of Figs. 7 and 8 suggests that perhaps an average of the two stress distributions may give a constant velocity profile. This is indeed found to be the case as shown in Fig. 9.

Because of long computing times, it is difficult to reach steady state on the computer. Instead, the impressing velocity (of the punch) is plotted versus the reciprocal time as shown in Fig. 10. The computer results are then fitted by multiple-order polynomials of reciprocal time to extrapolate to infinite time. It is seen that the extrapolated values agree reasonably well with experiments.

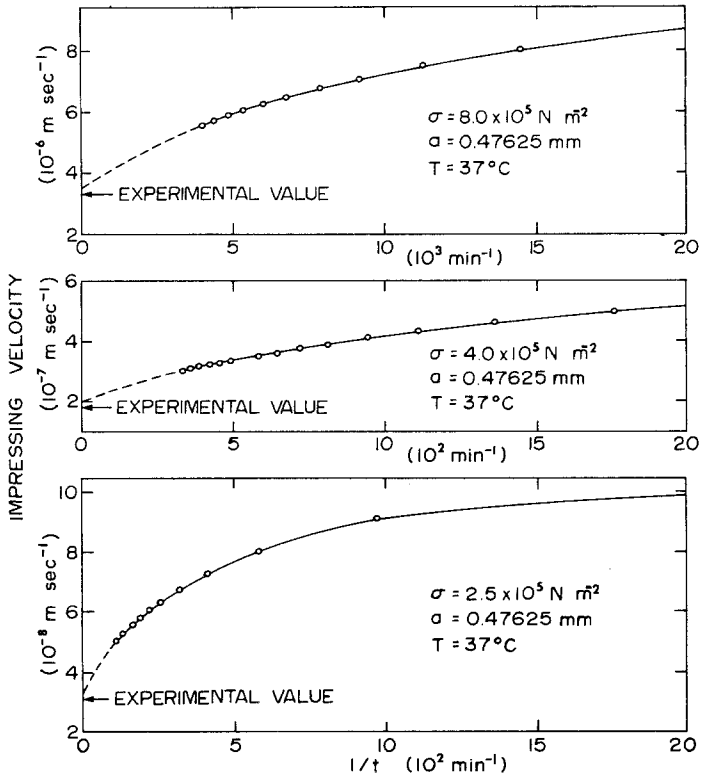

Figure 10 Polynomial curve fitting for the extrapolation to steady-state impressing velocities at three different punching stresses.

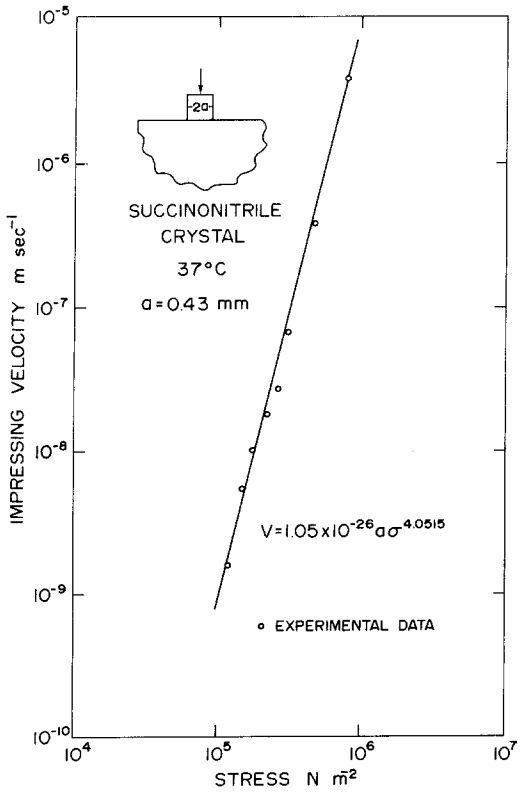

Figure 11 A comparison between calculated and experimental impressing velocities as a function of punching stress.

The stress dependence of impressing velocity at 37° C is shown in Fig. 11 together with some experimental data. The agreement seems satisfactory. From a dimensional analysis of Equation 17, it is obvious that for the same punching stress, the steady-state impressing velocity is proportional to the punch radius, as long as the specimen is sufficiently large compared to the punch. As shown in the previous paper, this punch size effect has been confirmed by experiment.

7. Summary and conclusions

(1) Finite element analysis is applied to impression creep testing. The potential energy of the system is minimized by holding creep strain constant. The creep strain distribution is based on von Mises flow rule. A power law constitutive equation between von Mises stress and creep rate is used for the deformation of each and every element. Some approximations are used to simplify the calculations.

(2) The elastic stresses calculated by the finite element analysis agree well with theoretical values of Terazawa and of Harding and Sneddon for the semi-infinite medium.

(3) For succinonitrile crystals, the impressing velocity calculated at several punching stresses and extrapolated to steady-state conditions agree very well with experimental values presented in the previous paper. The stress distribution under the punch during creep is adjusted so that the displacement velocity is uniform under the punch.

(4) This analysis establishes a power law between the steady-state impressing velocity and punching stress as a direct consequence of the same power law between steady-state creep and von Mises stress assumed for each element.

Acknowledgement

This work was supported by ERDA through contract EY-76-S-02-2296*000.

References

1. O. C. ZIENKIEWICZ, "The Finite Element Method in Engineering Science" (McGraw–Hill, London, 1971).
2. K. H. HUEBNER, "The Finite Element Method for Engineers" (Wiley, New York, 1975).
3. G. A. GREENBAUM and M. F. RUBINSTEIN, *Nucl. Eng. Design* 7 (1968) 379.
4. W. H. SUTHERLAND, *ibid* **11** (1970) 269.
5. H. FONTAINE and C. MORIAMEZ, *J. Chem. Phys.* **65** (1968) 969.
6. A. REUSS, *Z. Angew. Math. Mech.* **9** (1929) 49; W. VOIGT, Lehrbuch der Kristallphysik (Teubner, Leipsig, 1928) p. 410; see also R. F. S. HEARMON, "Introduction to Applied Anisotropic Elasticity" (Oxford University Press, Oxford, 1961) p. 41.
7. K. TERAZAWA, *J. College Sci. Imperial U. Tokyo* **37** (1916) Art. 7
8. J. W. HARDING and I. N. SNEDDON, *Proc. Cambridge Phil Soc.* **41** (1945) 16.

Received 18 February and accepted 11 March 1977.